Fusion Engineering and Design 96–97 (2015) 703–706

Contents lists available at ScienceDirect

Fusion Engineering and Design

journal homepage: www.elsevier.com/locate/fusengdes

A novel approach for solving three dimensional eddy current problems in fusion devices

Paolo Bettini[a,b], Ruben Specogna[c,*]

[a] Consorzio RFX, C.so Stati Uniti 4, 35127 Padova, Italy
[b] DII, Università di Padova, 35131 Padova, Italy
[c] DIEGM, Università di Udine, 33100 Udine, Italy

HIGHLIGHTS

- The solution of eddy current problems arising in fusion engineering is addressed.
- The numerical method exploits the symmetry that many fusion devices exhibit.
- It works even if field sources (plasma or external coils) do not share the domain symmetry.
- A substantial reduction of memory and computational time requirements is obtained.

ARTICLE INFO

Article history:
Received 26 September 2014
Received in revised form
17 November 2014
Accepted 3 December 2014
Available online 19 December 2014

Keywords:
Eddy currents
Cyclic symmetry
Fusion engineering and design

ABSTRACT

We present a technique to efficiently solve 3D eddy current problems in fusion devices, whose structures exhibit a geometrical symmetry. The proposed approach is based on the exploitation of symmetry via harmonic analysis and it is suitable to treat also problems where the field sources (plasma or external coils) do not share the domain symmetry. A simple test case is presented to describe the methodology. Then, a more complicated geometry is considered, which represents a realistic vacuum vessel of an ITER like fusion device (double layer structure with several portholes). The results are discussed for both axisymmetric and non-axisymmetric excitations in frequency domain.

1. Introduction

Many electromagnetic problems deal with symmetric structures (for example rotor/stator of a rotating electric machine). If the field sources share some symmetries, the overall problem can be reformulated on a restricted domain – the *symmetry cell* – by imposing suitable Boundary Conditions (BCs) [1], thus allowing a substantial reduction of memory and computational time requirements.

Also magnetic confinement fusion devices, presently operating or under construction, often exhibit a geometric symmetry of the structures which surround the plasma (e.g. vacuum vessel, stabilizing shells, plates or loops). For example, in ITER the main conducting structures can be modeled by gluing nine pieces of the same structure (*symmetry cell*), 40° wide in the toroidal direction. Unfortunately, such an effective approach is no longer valid whenever the field sources (plasma or external coils) do not share the domain symmetry.

Nevertheless, in many cases, it is still possible to take advantage of symmetries by reducing a given problem to a family of subproblems to be solved on the *symmetry cell*. Then, the global solution is build up by superposition of the partial results and application of symmetry operations [2]. The very idea is to use, in the framework of electromagnetic field analysis, a linear decomposition similar to the one adopted in the symmetrical component analysis of unbalanced three-phase power systems, originally introduced by Fortesque [3].

In this paper, we focus on the exploitation of symmetries for the solution of 3D eddy current problems in frequency domain. The electromagnetic problem is formulated according to the discrete geometric approach described in Section 2. An effective procedure to exploit the cyclic (rotational) symmetry (C_n, according to standard group theory definitions, see [4]) is presented in Section 3, together with a detailed description of its numerical implementation in the electromagnetic code *CAFE* [5]. Section 4 shows the

* Corresponding author. Tel.: +39 0432 55 8037.
E-mail address: ruben.specogna@uniud.it (R. Specogna).

http://dx.doi.org/10.1016/j.fusengdes.2014.12.002
0920-3796/

numerical results of the analysis carried out on two reference geometries: a thick flange with four holes (C_4 symmetry) and a more complicated geometry (C_{18} symmetry) which resembles a realistic vacuum vessel of a fusion device characterized by a double layer structure and 18 equatorial portholes. In both cases, axisymmetric and non-axisymmetric excitations are considered. Eventually, in Section 5, some conclusions are drawn.

2. Discrete geometric formulation

The eddy current problem is solved, in frequency domain, with a discrete geometric formulation which is based on the circulation of the magnetic vector potential over hexahedral grids [6]. The 3D domain of interest $\mathcal{D}$ is covered by a hexahedral mesh, whose incidences are encoded in the cell complex $\mathcal{K}$ represented by the standard incidence matrices **G**, **C** and **D** [7]. A dual barycentric complex $\tilde{\mathcal{K}}$ is obtained from $\mathcal{K}$ by using the *barycentric subdivision*; its incidence matrices are $\tilde{\mathrm{G}} = \mathbf{D}^T$, $\tilde{\mathrm{C}} = \mathbf{C}^T$ and $\tilde{\mathrm{D}} = -\mathbf{G}^T$ [7].

Three regions of $\mathcal{D}$ are identified: the passive conductive region $\mathcal{D}_c$ (including all conductive structures surrounding the plasma), the nonconductive region $\mathcal{D}_a$ (air or vacuum), and the source region $\mathcal{D}_s$ (active coils used to control the plasma instabilities).

By combining discrete Ampère's law and Faraday's law with the discrete counterpart of constitutive laws for the flux density **B** and the current density **J**, a symmetric complex linear system of equations is obtained [8],

$$\mathbf{K}\,\mathbf{A}_r = -i\omega\,\mathbf{M}_\sigma\,\mathbf{A}_s, \tag{1}$$

where ω is the angular frequency, $\mathbf{K} = \mathbf{C}^T\mathbf{M}_\nu\,\mathbf{C} + i\omega\,\mathbf{M}_\sigma$, $\mathbf{M}_\nu$ and $\mathbf{M}_\sigma$ are square material matrices that represent the discrete version of the constitutive laws. Material matrices are efficiently computed as described in [9]. The unknowns $\mathbf{A}_r$ are the circulations of the reduced magnetic vector potential along primal edges $e \in \mathcal{D}$ due to eddy currents in $\mathcal{D}_c$, only. On the right-hand side, $\mathbf{A}_s$ denotes the circulations of the magnetic vector potential along $e \in \mathcal{D}_c$ produced by the sources in $\mathcal{D}_s$ and zero for edges in $\mathcal{D}_a \bigcup \mathcal{D}_s$. Each entry of $\mathbf{A}_s$ can be computed with standard closed formulas. Then, the circulations of the modified magnetic vector potential **A** can be expressed as: $\mathbf{A} = \mathbf{A}_r + \mathbf{A}_s$.

3. Solution exploiting cyclic symmetry (C_n)

C_n group describes the rotational symmetry of order n around an axis (e.g. the z-axis in fusion devices):

$$C_n = \{1, r, r^2, \ldots, r^{n-1}\} \tag{2}$$

where $r = e^{i2\pi/n}$. It is referred to as *cyclic* due to the relation: $r^{n+p} = r^p$.

An example of domain (geometry) which exhibits a cyclic symmetry (C_4) is shown in Fig. 1: Σ is the *symmetry cell*; isometries r, r^2, and r^3 are the angle rotations equal to $\pi/2$, π and $3\pi/2$, respectively.

Let $\mathbf{b}_j^C$ denotes the right-hand side relative to the jth substructure and $\mathbf{K}^C$ the system matrix of the symmetry cell. Here we provide the recipe to solve (1) by solving n uncoupled problems on the symmetry cell.

1 A tree–cotree gauge is used to minimize the unknowns and to obtain a full-rank system. During the tree construction it is wise not to include as tree edges the ones on the symmetry surfaces S_1 and S_2 of the symmetry cell. This generates a tree gauge which enables the enforcement of the Pseudo-Periodic Boundary Conditions (PPBCs) at step 3.

2 Compute the right-hand side of the kth system with

$$\mathbf{b}^k = \frac{1}{n}\sum_{j=0}^{n-1} e^{-i(2\pi/n)jk}\,\mathbf{b}_j^C, \tag{3}$$

where $k = 1, \ldots, n-1$.

3 Solve

$$\mathbf{K}^C\mathbf{A}_r^k = \mathbf{b}^k \tag{4}$$

subject to the following PPBCs on S_1 and S_2

$$\mathbf{A}_{r,f}^k = e^{i(2\pi/n)k}\,\mathbf{A}_{r,e}^k, \tag{5}$$

where edge $e \in S_1$ and f is the corresponding edge on S_2[1].

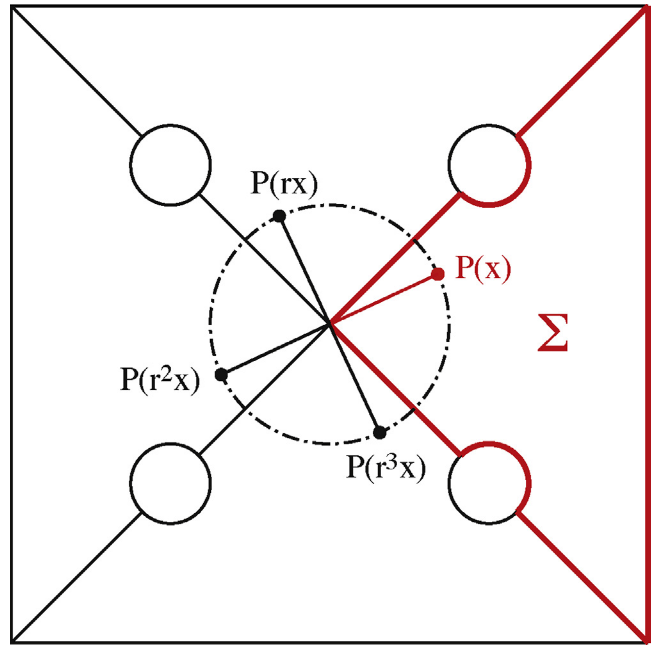

Fig. 1. An example of geometry which exhibits a cyclic symmetry (C_4). Σ is the *symmetry cell*. Isometries r, r^2, r^3 are the angle rotations equal to $\pi/2$, π and $3\pi/2$, respectively.

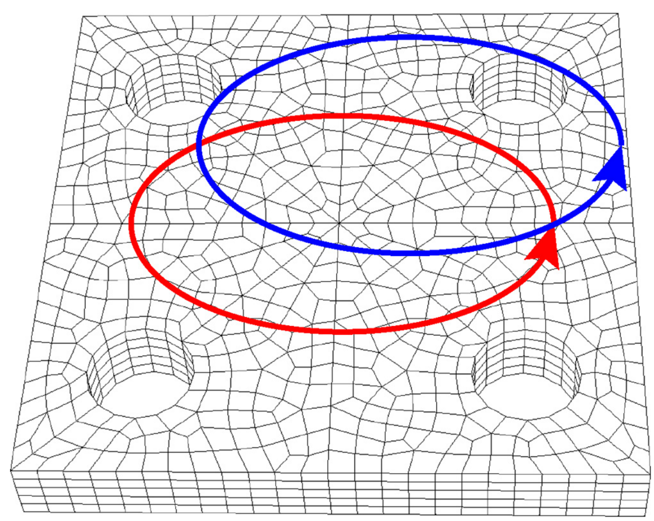

Fig. 2. First geometry of passive conductive region $\mathcal{D}_c$ (C_4 symmetry, 90° *symmetry cell*): a thick flange with four holes. The numerical domain $\mathcal{D}$ is discretised in 15,195 hexahedra, 16,736 nodes and 48,618 edges. An example of axisymmetric (red) and non-axisymmetric (blue) field sources are also shown. (For interpretation of the references to colour in this figure legend, the reader is referred to the web version of this article.)

[1] This is easily implemented during the assembly. In fact, contributions from edges on S_1 are assembled unaltered, whereas the ones from edges on S_2 are assembled, multiplied by $e^{2i\pi k/n}$, in the positions relative to the corresponding edges on S_1.

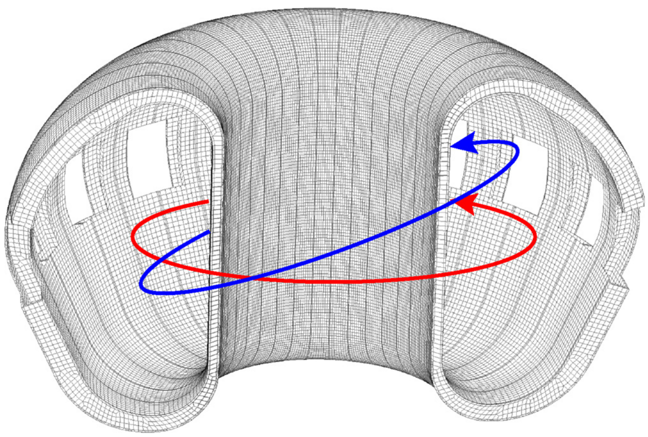

Fig. 3. Second geometry of passive conductive region $\mathcal{D}_c$ (C_{18} symmetry, 20° *symmetry cell*): an example of vacuum vessel (ITER-like machine). The numerical domain $\mathcal{D}$ (only one half is shown) is discretised in 3,414,888 hexahedra, 3,426,237 nodes and 10,267,062 edges. Red/blue current loops mimic an axisymmetric/non-axisymmetric plasma current. (For interpretation of the references to colour in this figure legend, the reader is referred to the web version of this article.)

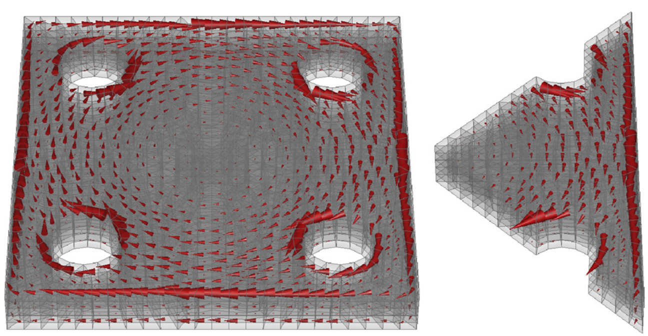

Fig. 4. Eddy current plot (red cones: real part of **J**, not to scale). Axisymmetric excitation (centered current loop, AC, f = 100 Hz). Left: standard solution on the entire domain. Right: solution by exploiting C_4 symmetry. (For interpretation of the references to colour in this figure legend, the reader is referred to the web version of this article.)

4 Extend each solution to the whole domain

$$\mathrm{A}_r^k = \left[\mathbf{A}_r^k, e^{i2\pi/n}\mathbf{A}_r^k, \ldots, e^{i2\pi(n-1)/n}\mathbf{A}_r^k\right]^T \tag{6}$$

and reconstruct the solution with

$$\mathbf{A}_r = \sum \mathrm{A}_r^k. \tag{7}$$

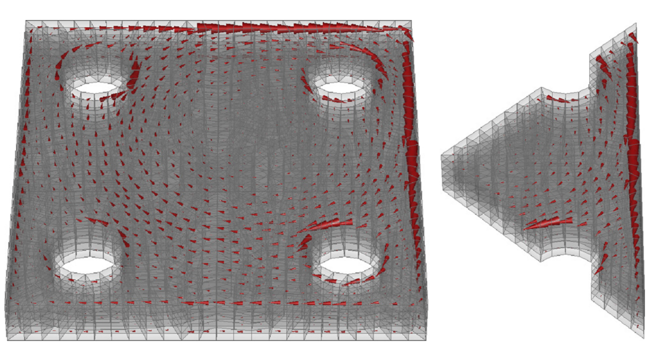

Fig. 5. Eddy current plot (red cones: real part of **J**, not to scale). Non-axisymmetric excitation (not centered current loop, AC, f = 100 Hz). Left: standard solution on the entire domain. Right: solution on the *symmetry cell* calculated by exploiting C_4 symmetry. The solution in the other 90° cells can be obtained by (6) and (7). (For interpretation of the references to colour in this figure legend, the reader is referred to the web version of this article.)

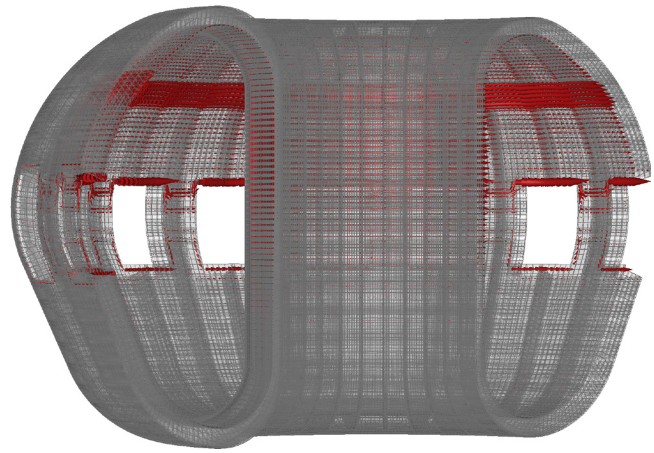

Fig. 6. Axisymmetric field source: current loop (1 MA, 100 Hz) centered at [*x* = *y* = *0*, *z* = *2m*]. Results calculated on the entire domain (360°). Red cones: real part of J, not to scale. (For interpretation of the references to colour in this figure legend, the reader is referred to the web version of this article.)

4. Numerical results

The proposed approach has been applied to calculate the eddy current induced in two reference conducting structures, excited by external AC fields:

1 A thick flange with four holes (C_4 symmetry, 90° *symmetry cell*, see Fig. 2).
2 A structure which resembles the vacuum vessel of an ITER-like device (C_{18} symmetry, 20° *symmetry cell*, see Fig. 3), characterized by a double layer structure with stiffening ribs and 18 equatorial portholes evenly distributed toroidally.

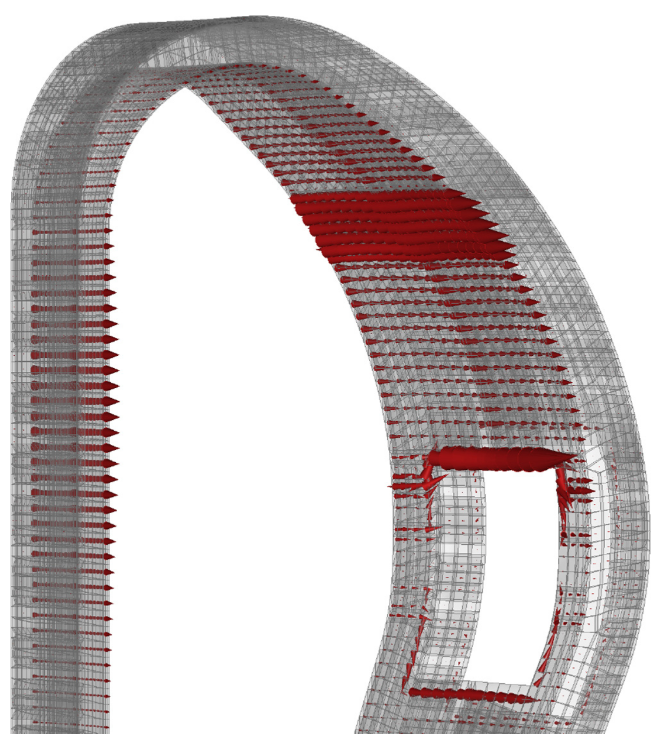

Fig. 7. Axisymmetric field source: current loop (1 MA, 100 Hz) centered at [*x* = *y* = *0*, *z* = *2m*]. A detail of the solution calculated on the *symmetry cell* exploiting C_{18} symmetry. The solution in the other 20° cells can be obtained by (6)–(7). Red cones: real part of J, not to scale. (For interpretation of the references to colour in this figure legend, the reader is referred to the web version of this article.)

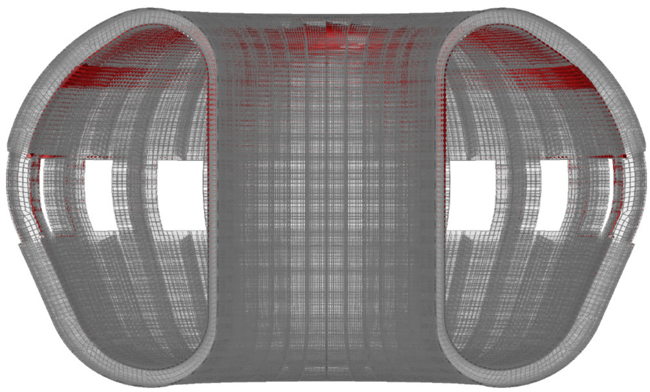

Fig. 8. Non-axisymmetric field source: current loop (1 MA, 100 Hz) centered at [$x = 0$, $y = 1m$, $z = 2m$], tilt $\alpha = 10^{\circ}$ around *x-axis*. Results calculated on the entire domain (360°). Red cones: real part of J, not to scale. (For interpretation of the references to colour in this figure legend, the reader is referred to the web version of this article.)

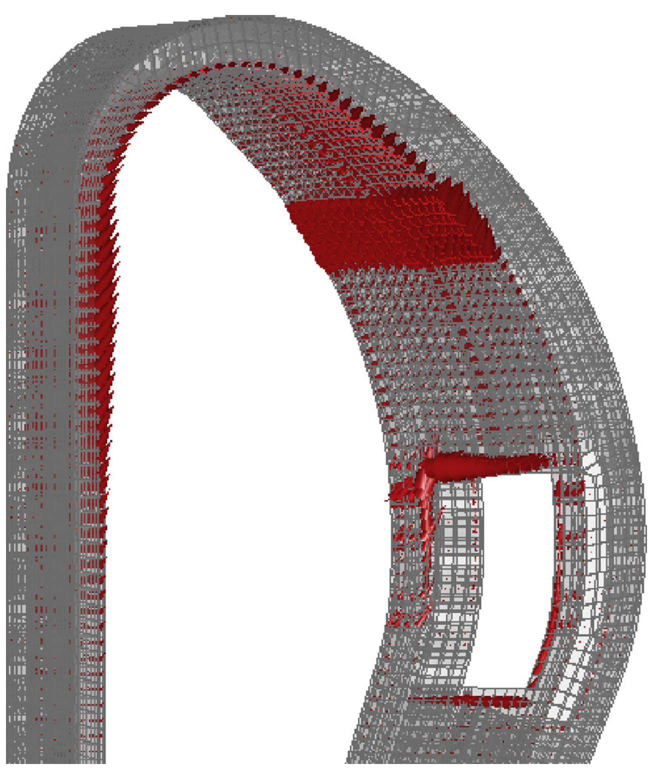

Fig. 9. Non-axisymmetric field source: current loop (1 MA, 100 Hz) centered at [$x = 0$, $y = 1m$, $z = 2m$], tilt $\alpha = 10^{\circ}$ around *x-axis*. A detail of the solution calculated on the *symmetry cell* exploiting C_{18} symmetry. The solution in the other 20° cells can be obtained by (6) and (7). Red cones: real part of J, not to scale. (For interpretation of the references to colour in this figure legend, the reader is referred to the web version of this article.)

A comparison between the standard approach (solution on the entire domain) and new approach (exploitation of symmetry) is presented. The eddy currents induced in the first geometry under axisymmetric (centered current loop) or non-axisymmetric (not centered current loop) excitations are shown in Figs. 4 and 5, respectively. The results are in excellent agreement.

Then, the second geometry has been considered. Again, a comparison between standard and new approaches is presented. Both axisymmetric and non-axisymmetric excitations are considered (current loops which mimic the plasma current). The results are presented in Figs. 6–9, respectively. An excellent agreement is found with a substantial reduction of memory and computational time requirements. In fact, the solution of the problem on the entire domain (≈7.2 million unknowns) takes 5300 s, while the solution on the *symmetry cell* (solution of 18 subproblems with ≈380 thousand unknowns each) takes 400 s on a workstation equipped with two 8-core Xeon processors (2.7 GHz).

5. Conclusions

An effective approach for the solution of 3D eddy current problems in frequency domain has been presented. The proposed approach is based on the exploitation of symmetry via harmonic analysis and it is suitable to treat also problems where the field sources (plasma or external coils) do not share this symmetry, allowing a substantial reduction of memory and computational time requirements. Two reference test cases have been presented and the numerical results discussed.

Acknowledgment

This work was partially supported by the Italian MIUR under PRIN grant 2010SPS9B3.

References

[1] A. Bossavit, Symmetry, groups, and boundary value problems. A progressive introduction to noncommutative harmonic analysis of partial differential equations in domains with geometrical symmetry, Comput. Methods Appl. Mech. Eng. 56 (1986) 167–215.
[2] A. Bossavit, Boundary value problems with symmetry, and their approximation by finite elements, SIAM J. Appl. Math. 53 (1993) 1352–1380.
[3] C.I. Fortescue, Method of symmetrical coordinates applied to the solution of polyphase networks, AIEE Trans. 37 (1918) 1027–1140.
[4] J.P. Serre, Linear Representations of Finite Groups, Springer-Verlag, Berlin, 1977.
[5] P. Bettini, R. Specogna, Computation of stationary 3D halo currents in fusion devices with accuracy control, J. Comput. Phys. 273 (2014) 100–117.
[6] P. Bettini, L. Marrelli, R. Specogna, Calculation of 3D magnetic fields produced by MHD active control systems in fusion devices, IEEE Trans. Magn. 50 (2) (2014) 7000904.
[7] E. Tonti, The Mathematical Structure of Classical and Relativistic Physics, Birkhäuser, Basel, 2013.
[8] A. Pirani, M. Ricci, R. Specogna, A. Tamburrino, F. Trevisan, Multi-frequency identification of defects in conducting media, Inverse Probl. 24 (2008) 035011.
[9] L. Codecasa, R. Specogna, F. Trevisan, A new set of basis functions for the discrete geometric approach, J. Comput. Phys. 229 (2010) 401–410.